17th World Conference on Earthquake Engineering, 17WCEE
Sendai, Japan - September 13th to 18th 2020
Paper N° C001222
Registration Code: S-A02955

A SYSTEMATIC APPROACH TO SOLVE THE VEHICLE-BRIDGE INTERACTION PROBLEM UNDER EARTHQUAKE

C.D. Stoura [1], E. Paraskevopoulos [2], E.G. Dimitrakopoulos[3]

[1] *Ph.D. candidate, Department of Civil and Environmental Engineering, Hong Kong University of Science and Technology, Clear Water Bay, Kowloon, Hong Kong, cstoura@connect.ust.hk*
[2] *Post-doctoral fellow, Department of Mechanical Engineering, Aristotle University of Thessaloniki, 54 124, Thessaloniki, Greece, eapcivil@gmail.com*
[3] *Associate Professor, Department of Civil and Environmental Engineering, Hong Kong University of Science and Technology, Clear Water Bay, Kowloon, Hong Kong, ilias@ust.hk*

Abstract

This paper presents an original scheme to solve the vehicle-bridge interaction (VBI) problem under seismic excitation in a complete and systematic manner. Specifically, the proposed methodology relies upon the localized Lagrange multipliers approach, a method that partitions the vehicle and the bridge systems by introducing auxiliary contact points between the two subsystems, and also incorporates fundamental concepts of differential geometry based on the invariance of a generalized form of Newton's law of motion when imposing bilateral motion constraints. This approach leads to a dynamic representation of the constraint equations and the associated Lagrange multipliers. The study considers a synchronous (uniform) seismic excitation on the vehicle-bridge system. This method leads to several potential advantages. Firstly, all equations describing the mechanical system — equations of motion and constraint equations — are expressed as a set of second-order differential equations (ODEs), both for the generalized coordinates and the Lagrange multipliers, avoiding constraint drifts and singularities commonly associated with differential-algebraic equations (DAEs). As a result, there is no need to impose additional numerical stabilization techniques, such as Baumgarte stabilization, projections, etc.. At the same time, it provides a theoretical insight into the equations derived and, subsequently, a direct comparison with commonly adopted formulas to solve the coupled VBI problem. Lastly, it sets the basis for the development of robust numerical analysis schemes to integrate the VBI problem, based on a solid theoretical framework.

Keywords: vehicle-bridge interaction; dynamic Lagrange multipliers; seismic response; numerical stability

1. Introduction

The rapid expansion of high-speed railway (HSR) systems worldwide and the increasing ratio of HSR lines made up of bridges [1] create the incentive to revisit the dynamic interaction between HSR trains and bridges [2]. Especially under seismic excitations, dynamic vehicle-bridge interaction (VBI) intensifies [2], threatening, in some cases, the safety of transportation [[3]-[4]].

The solution of the seismic VBI (SVBI) problem involves the application of robust VBI algorithms [[5]-[9]] to coupled vehicle-bridge systems subjected to seismic motions. Yang et al. [10] solved the SVBI problem using a dynamic condensation method that condenses the degrees of freedom (DOFs) of the vehicle to those of the bridge. This method applies the earthquake excitation as a uniform external force to the system. Zeng and Dimitrakopoulos [3] investigated the SVBI problem under uniform seismic excitations, adopting their previously developed algorithm for vehicles running on curved bridges [6]. This method [3] also takes into account creep forces due to rolling contact, which under earthquakes excitations can become significant. Xia et al. [11] solved the SVBI problem via an iterative approach that solves the vehicle and bridge subsystems separately [8] and imposes earthquakes via an influence matrix that applies different seismic load at each support of the bridge. Du et al. [12] followed a similar approach [11] but applied seismic excitation on the bridge as asynchronous displacements of the ground at the supports.

Algorithms to solve mechanical systems subjected to motion constraints, such as coupled vehicle-bridge systems, often encounter stability problems associated with Differential-Algebraic Equations (DAEs) [13]. These lead to numerical drifts during the time-integration [14]. A typical approach to overcome numerical instabilities is the adoption of stabilization techniques, such as Baumgarte stabilization and projections [14]. However, such methods lack a solid theoretical background. Aiming at the systematic and consistent definition of the kinematic constraints of mechanical systems, Natsiavas and Paraskevopoulos [15] proposed a dynamic treatment of Lagrange multipliers associated with motion constraints. This approach [15] relies on the invariance of a generalized form of Newton's law of motion when imposing bilateral constraints [16]. As a result, both generalized coordinates and Lagrange multipliers constitute a set of second-order Ordinary Differential Equations (ODEs). Therefore, there is no need to introduce artificial terms to stabilize the system, which is common in multibody dynamics area [17].

Building on the work of Zeng et al. [9] and Natsiavas and Paraskevopoulos [15], this study proposes an original approach to solve the SVBI problem. Based on a localized Lagrange multipliers approach [9] that solves the VBI problem in a partitioned manner, this method introduces auxiliary contact points between the vehicle and the bridge. Also, it treats Lagrange multipliers dynamically via ODEs [15], avoiding instabilities that arise by the solution of high-index DAEs. Lastly, it applies seismic excitation at the supports of the bridge via kinematic constraints with the ground, handling efficiently synchronous, as well as, asynchronous excitations. The proposed algorithm solves the SVBI problem in a consistent, precise and efficient manner.

2. Seismic vehicle-bridge interaction system modelling

The study partitions the coupled vehicle-bridge system by introducing auxiliary contact points between the vehicle's wheels and the bridge (Fig. 1(a)), similar to the study of Zeng et al. [9]. This method leads to the assignment of two sets of Lagrange multipliers corresponding to the vehicle and bridge subsystems, respectively. Subsequently, the two subsystems can be solved separately, decreasing the computational cost of the analysis significantly. The proposed scheme treats the auxiliary contact points as an intermediate system (between the vehicle and the bridge), consisting of masses proportional to the vehicle's wheels mass (Fig 1(a)). The three systems (vehicle, bride and auxiliary contact points) are connected through kinematic constraints in the normal direction.

A distinctive characteristic of the proposed approach is the consistent application of Newton's law in order to formulate the motion constraints [15]. The Lagrange multipliers are treated similarly to the generalized coordinates of the system, which allows the assignment of appropriate inertia, damping and stiffness to each

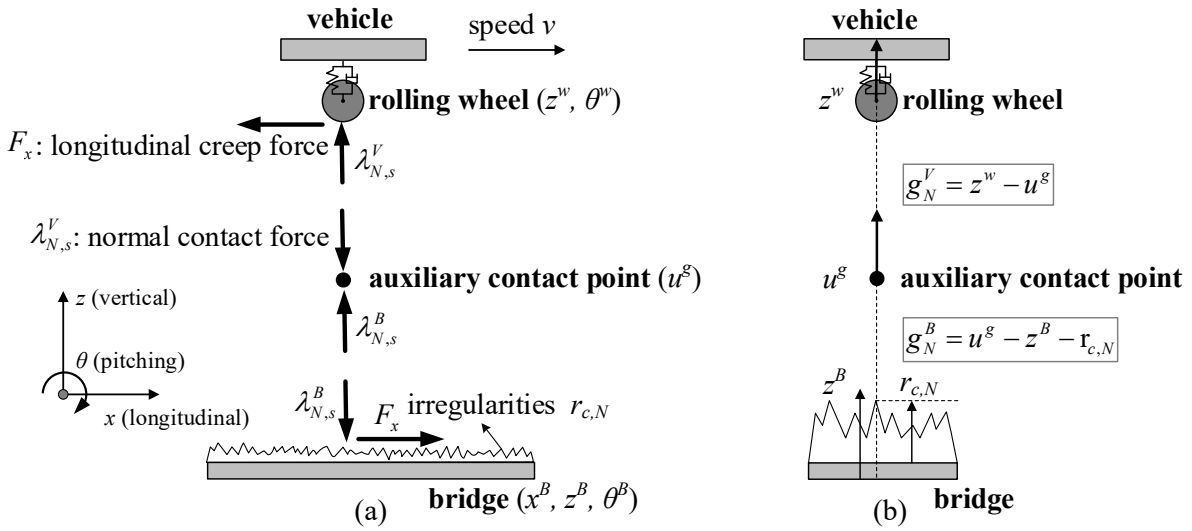

Fig. 1 – Vehicle-bridge contact model in the normal and tangential directions according to the proposed partitioned algorithm: (a) contact forces and (b) gap functions.

each one of the constraints [15]. This approach leads to the formulation of a set of second-order ODEs for both the generalized coordinates and Lagrange multipliers. The study treats the earthquake excitation in a similar manner, i.e., as a set of constraints at the bridge supports.

In this study, the equations of motion and constraint equations constitute a system of ODEs as follows:

$$\mathbf{S}_I \left[\mathbf{u}^V \quad \mathbf{u}^B \quad \boldsymbol{\lambda}^V_N \quad \boldsymbol{\lambda}^B_N \quad \mathbf{u}^g \quad \boldsymbol{\lambda}^{B,g} \right]^{\mathrm{T}} = \mathbf{F}^{\mathrm{T}} . \tag{1}$$

In Eq. (1), $\mathbf{S}_I$ is a differential operator, including mass, damping and stiffness properties of the system. $\mathbf{u}$ denotes displacement vectors and $\boldsymbol{\lambda}$ Lagrange multiplier vectors. Superscript V corresponds to the vehicle, B to the bridge and g to the ground. Supersctipt T denotes the inverse of a vector or matrix. Vector $\mathbf{F}$ at the right-hand side of Eq. (1) involves external and creep forces acting on the system. All parameters of Eq. (1) are explained in detail in the following sections (Sections 2 and 3).

2.1 Vehicle modelling

As a first approach, consider a two-dimensional (2D) vehicle model (Fig. 2). The vehicle model is a multi-body assembly consisting of seven rigid bodies (one car-body, two bogies and four wheelsets) connected with linear springs and dashpots. All bodies are assigned two DOFs each, one translation and one rotation:

$$\mathbf{u}^u = \left[z^u \quad \theta^u \right] \tag{2}$$

where y^u and z^u are the lateral and vertical translations, and ψ^u, φ^u and θ^u correspond to the yawing, rolling and pitching Euler angles, respectively. Superscript u denotes the vehicle's car-body for $u = c$, while $u = t1$, $t2$ denotes the front and rear bogies, respectively. Lastly, $u = wi$ corresponds to each one of the wheels, where i = 1-4. The longitudinal DOF is eliminated for all bodies, assuming constant moving speed v. Thus, in total, the vehicle has 14 DOFs. The displacement vector $\mathbf{u}^V$ of the entire vehicle system is:

$$\mathbf{u}^V = \left[\mathbf{u}^c \quad \mathbf{u}^{t1} \quad \mathbf{u}^{t2} \quad \mathbf{u}^{w1} \quad \mathbf{u}^{w2} \quad \mathbf{u}^{w3} \quad \mathbf{u}^4 \right]^{\mathrm{T}} . \tag{3}$$

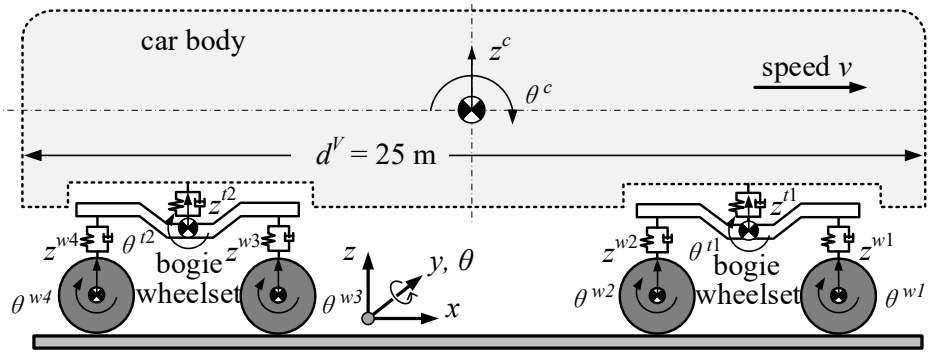

Fig. 2 – 14-DOF vehicle model

Assuming rigid contact between the auxiliary contact points and vehicle's wheels in the normal direction [9], the equation of motion (EOM) of the vehicle system is:

$$\tilde{\mathbf{m}}^V \ddot{\mathbf{u}}^V + \mathbf{c}^V \dot{\mathbf{u}}^V + \mathbf{k}^V \mathbf{u}^V = \mathbf{F}^V - \mathbf{W}_N^V \boldsymbol{\lambda}_{N,s}^V - \mathbf{W}_T^V \mathbf{F}_x \tag{4}$$

where $\tilde{\mathbf{m}}^V$, $\mathbf{c}^V$ and $\mathbf{k}^V$ are the vehicle mass, damping and stiffness matrices, and $\mathbf{F}^V$ is the external force vector acting on the vehicle. $\boldsymbol{\lambda}_{N,s}^V \in \Re^{4\times 1}$ is the contact force vector between the vehicle's wheels and the auxiliary contact points in the normal direction. In the tangential direction, the study assumes rolling contact between the wheels and the rails, which generates longitudinal creep forces $\mathbf{F}_x \in \Re^{4\times 1}$. $\mathbf{W}_N^V \in \Re^{14\times 4}$ and $\mathbf{W}_T^V \in \Re^{14\times 4}$ are the vehicle's contact direction matrices in the normal and tangential directions, respectively [9]. Following the approach of Zeng and Dimitrakopoulos [9], Eq. (4) can be written as:

$$\mathbf{K}_{\text{eff}}^V \mathbf{u}^V = \mathbf{F}^V - \mathbf{W}_N^V \boldsymbol{\lambda}_{N,s}^V - \mathbf{W}_T^V \mathbf{F}_x \tag{5}$$

where $\mathbf{K}_{\text{eff}}^V$ is the effective stiffness of the vehicle, defined as:

$$\mathbf{K}_{\text{eff}}^V = \tilde{\mathbf{m}}^V \frac{d^2}{dt^2} + \mathbf{c}^V \frac{d}{dt} + \mathbf{k}^V . \tag{6}$$

$\frac{d}{dt}$ denotes differentiation with respect to time. Formulating the Lagrange multipliers in the normal direction as ODEs, and assigning proper mass, damping and stiffness to the constraints according to the study of Natsiavas and Paraskevopoulos [15], $\boldsymbol{\lambda}_{N,s}^V$ becomes:

$$\boldsymbol{\lambda}_{N,s}^V = \bar{\mathbf{m}}_N^V \ddot{\boldsymbol{\lambda}}_N^V + \bar{\mathbf{c}}_N^V \dot{\boldsymbol{\lambda}}_N^V + \bar{\mathbf{k}}_N^V \boldsymbol{\lambda}_N^V . \tag{7}$$

$\bar{\mathbf{m}}_N^V$, $\bar{\mathbf{c}}_N^V$ and $\bar{\mathbf{k}}_N^V$ are the mass, damping and stiffness matrices of the contact constraints between the vehicle and the auxiliary contact points in the normal direction, defined later in Section 3. Rewriting Eq. (5) with the aid of Eq. (7), the EOM of the vehicle becomes:

$$\mathbf{K}_{\text{eff}}^V \mathbf{u}^V = \mathbf{F}^V - \mathbf{W}_N^V \bar{\mathbf{K}}_{\text{eff},N}^V \boldsymbol{\lambda}_N^V - \mathbf{W}_T^V \mathbf{F}_x \tag{8}$$

with $\bar{\mathbf{K}}_{\text{eff},N}^V$ being the effective stiffness of the constraints, defined as:

$$\bar{\mathbf{K}}_{\text{eff},N}^{V} = \bar{\mathbf{m}}_{N}^{V} \frac{d^2}{dt^2} + \bar{\mathbf{c}}_{N}^{V} \frac{d}{dt} + \bar{\mathbf{k}}_{N}^{V} . \tag{9}$$

2.2 Bridge modelling

The bridge is modelled with the Finite Element Method (FEM), assuming two-dimensional (2D) Euler-Bernoulli beams. The auxiliary contact points are in rigid contact with the bridge in the normal direction [9]. Similar to the vehicle EOM (Eq. (8)), the bridge EOM can be written as:

$$\mathbf{K}_{\text{eff}}^{B} \mathbf{u}^{B} = \mathbf{F}^{B} + \mathbf{W}_{N}^{B} \bar{\mathbf{K}}_{\text{eff},N}^{B} \boldsymbol{\lambda}_{N}^{B} + \mathbf{W}_{T}^{B} \mathbf{F}_{x} + \mathbf{E}^{B,g} \bar{\mathbf{K}}_{\text{eff}}^{B,g} \boldsymbol{\lambda}^{B,g} \tag{10}$$

where $\mathbf{u}^{B}$ is the bridge response vector and $\mathbf{K}_{\text{eff}}^{B}$ is the effective stiffness of the bridge, defined as:

$$\mathbf{K}_{\text{eff}}^{B} = \mathbf{m}^{B} \frac{d^2}{dt^2} + \mathbf{c}^{B} \frac{d}{dt} + \mathbf{k}^{B} . \tag{11}$$

$\mathbf{m}^{B}$, $\mathbf{c}^{B}$ and $\mathbf{k}^{B}$ are the mass, damping and stiffness matrices and $\mathbf{F}^{B}$ is the external force vector acting on the bridge. $\mathbf{W}_{N}^{B} \in \Re^{\text{DOF}^{\text{B}} \times 4}$ is the bridge's contact direction matrix in the normal direction, corresponding to the contact force vector $\boldsymbol{\lambda}_{N}^{B} \in \Re^{4\times 1}$, and $\mathbf{W}_{T}^{B} \in \Re^{\text{DOF}^{\text{B}} \times 4}$ is the contact direction matrix in the tangential direction corresponding to the creep force vector $\mathbf{F}_{x} \in \Re^{4\times 1}$. Both $\mathbf{W}_{N}^{B}$ and $\mathbf{W}_{T}^{B}$ contain linear shape functions for the axial DOFs and cubic (Hermitian) shape functions for the flexural DOFs. DOF^{B} denotes the number of DOFs of the bridge. $\bar{\mathbf{K}}_{\text{eff},N}^{B}$ is the effective stiffness of the constraints in the normal direction:

$$\bar{\mathbf{K}}_{\text{eff},N}^{B} = \bar{\mathbf{m}}_{N}^{B} \frac{d^2}{dt^2} + \bar{\mathbf{c}}_{N}^{B} \frac{d}{dt} + \bar{\mathbf{k}}_{N}^{B} . \tag{12}$$

where $\bar{\mathbf{m}}_{N}^{B}$, $\bar{\mathbf{c}}_{N}^{B}$ and $\bar{\mathbf{k}}_{N}^{B}$ are, respectively, the mass, damping and stiffness matrices of the contact constraints. $\mathbf{E}^{B,g}$ is the matrix of the constraints at the bridge supports due to earthquake motion. $\boldsymbol{\lambda}^{B,g}$ is the pertinent Lagrange multipliers vector and $\bar{\mathbf{K}}_{\text{eff}}^{B,g}$ is the corresponding effective stiffness defined as:

$$\bar{\mathbf{K}}_{\text{eff}}^{B,g} = \bar{\mathbf{m}}^{B,g} \frac{d^2}{dt^2} + \bar{\mathbf{c}}^{B,g} \frac{d}{dt} + \bar{\mathbf{k}}^{B,g} \tag{13}$$

where $\bar{\mathbf{m}}^{B,g}$, $\bar{\mathbf{c}}^{B,g}$ and $\bar{\mathbf{k}}^{B,g}$ are the mass, damping and stiffness matrices of the seismic motion constraints.

2.3 Auxiliary contact points

The study solves the coupled problem in a partitioned manner by introducing auxiliary contact points between the vehicle and bridge subsystems. The displacement vector of the auxiliary contact points $\mathbf{u}^{g}(t) \in \Re^{4\times 1}$ includes translational DOFs in the normal direction, where a "rigid contact" kinematic constraint is applied. Rigid contact assumes continuous contact between the wheels and the bridge [9].

This study considers the auxiliary contact points as an intermediate system, between the vehicle and the bridge, with mass $\mathbf{m}^{g}$ proportional to that of the vehicle's original mass $\mathbf{m}^{V}$. Therefore, it introduces a coefficient a to share $\mathbf{m}^{V}$ between the wheels and contact points. The values of a should be such that: a) the mass of the vehicle's wheels does not become negative and b) the total mass of the system (and thus the system dynamics) does not change. Consequently, $0 < a < 1$. Also, by eliminating the equation of motion of the auxiliary contact points (Eq. (14)) and the corresponding kinematic constraints (Eqs. (19) and (20) later), the equations of motion and kinematic constraints should coincide with those of the original vehicle-bridge

system. Thus, the mass matrix $\mathbf{m}^g$ of the auxiliary contact points is $\mathbf{m}^g = a\left(\mathbf{W}^V\right)^{\mathrm{T}} \mathbf{m}^V \mathbf{W}^V$, with $0 < a < 1$, and the corresponding active mass matrix of the vehicle is $\tilde{\mathbf{m}}^V = \mathbf{m}^V - \mathbf{m}^g \mathbf{W}^V \left(\mathbf{W}^V\right)^{\mathrm{T}}$ (Eq. (4)). For this simple 2D system, the mass of each contact point is $m^g = am^w$, and the active mass of each wheel becomes accordingly $\tilde{m}^w = (1-a)m^w$. The equation of motion of the auxiliary contact points is:

$$\mathbf{m}^g \frac{d^2}{dt^2}\mathbf{u}^g = \mathbf{F}^g + \mathbf{E}_N^V \bar{\mathbf{K}}_{\mathrm{eff},N}^V \boldsymbol{\lambda}_N^V - \mathbf{E}_N^B \bar{\mathbf{K}}_{\mathrm{eff},N}^B \boldsymbol{\lambda}_N^B \tag{14}$$

where $\mathbf{F}^g$ is the external force vector and $\mathbf{E}_N^V$, $\mathbf{E}_N^B$ are identity matrices pertaining to the vehicle and bridge subsystems, respectively.

2.4 Creep force model

The contact model in the tangential direction assumes rolling contact between the wheels and the bridge, which generates creep forces [3]. The calculation of creep forces follows the Kalker's creep model [18]. To account for high creepage during an earthquake, the creep force model considers a non-linear relationship between the creepage and the creep forces [19]. For a single wheel w*i*, the creep force vector is:

$$F_x^i = f_T^i \xi_T^i \tag{15}$$

where F_x^i is the creep force of wheel wi and ξ_T^i is the corresponding creepage. $f_T^i = -\varepsilon f_{33}$ is a creepage coefficient and ε^i is a saturation coefficient [19]. The creepage vector $\boldsymbol{\xi}_T$ (Eq. (12)) contains the normalized relative velocity between the wheels and the bridge and can be written as:

$$\boldsymbol{\xi}_T = \frac{1}{v}\left(\left(\mathbf{W}_T^V\right)^{\mathrm{T}} \frac{d}{dt}\mathbf{u}^V + v - \left(\mathbf{W}_T^B\right)^T \frac{d}{dt}\mathbf{u}^B - v\left(\mathbf{W}_T^B\right)'^T \mathbf{u}^B - v\mathbf{r}'_{c,T}\right) \tag{16}$$

where $\mathbf{r}_{c,T}$ is the rail irregularities vector in the tangential direction.

3. Kinematic constraints

In order to avoid problems related to DAEs, this study formulates both generalized coordinates and dynamic Lagrange multipliers through second-order ODEs. These equations represent the developed forces when the kinematic constraints tend to be violated [16].

3.1 Vehicle and bridge constraints

The kinematic constraint between the vehicle subsystem and the auxiliary contact points in the normal direction (Fig. 1(b)) is:

$$\bar{\mathbf{m}}_N^V \ddot{\mathbf{g}}_N^V + \bar{\mathbf{c}}_N^V \dot{\mathbf{g}}_N^V + \bar{\mathbf{k}}_N^V \mathbf{g}_N^V = \mathbf{0}. \tag{17}$$

where $\mathbf{g}_N^V$ is the gap function between the vehicle's wheels and the auxiliary contact points in the normal direction (Fig. 1(b)):

$$\mathbf{g}_N^V = \left(\mathbf{W}_N^V\right)^{\mathrm{T}} \mathbf{u}^V - \left(\mathbf{E}_N^V\right)^{\mathrm{T}} \mathbf{u}^g. \tag{18}$$

Substituting Eq. (18) into Eq. (17), the kinematic constraint becomes:

$$\bar{\mathbf{K}}_{\text{eff},N}^{V}\left[\left(\mathbf{W}_{N}^{V}\right)^{\mathrm{T}}\mathbf{u}^{V}-\left(\mathbf{E}_{N}^{V}\right)^{\mathrm{T}}\mathbf{u}^{g}\right]=\mathbf{0}. \tag{19}$$

Accordingly, for the bridge subsystem, the kinematic constraint with the auxiliary contact points in the normal direction is (Fig. 1(b)):

$$-\bar{\bar{\mathbf{K}}}_{\text{eff},N}^{B}\mathbf{u}^{B}+\bar{\mathbf{K}}_{\text{eff},N}^{B}\left(\mathbf{E}_{N}^{B}\right)^{\mathrm{T}}\mathbf{u}^{g}=v^{2}\bar{\mathbf{m}}_{N}^{B}\mathbf{r}_{c,N}''+v\bar{\mathbf{c}}_{N}^{B}\mathbf{r}_{c,N}'+\bar{\mathbf{k}}_{N}^{B}\mathbf{r}_{c,N} \tag{20}$$

with:

$$\bar{\bar{\mathbf{K}}}_{\text{eff},N}^{B}=\bar{\mathbf{m}}_{N}^{B}\left(\mathbf{W}_{N}^{B}\right)^{\mathrm{T}}\frac{d^{2}}{dt^{2}}+\left[2v\bar{\mathbf{m}}_{N}^{B}\left(\mathbf{W}_{N}^{B\prime}\right)^{\mathrm{T}}+\bar{\mathbf{c}}_{N}^{B}\left(\mathbf{W}_{N}^{B}\right)^{\mathrm{T}}\right]\frac{d}{dt}+v^{2}\bar{\mathbf{m}}_{N}^{B}\left(\mathbf{W}_{N}^{B\prime\prime}\right)^{\mathrm{T}}+v\bar{\mathbf{c}}_{N}^{B}\left(\mathbf{W}_{N}^{B\prime}\right)^{\mathrm{T}}+\bar{\mathbf{k}}_{N}^{B}\left(\mathbf{W}_{N}^{B}\right)^{\mathrm{T}}. \tag{21}$$

$\mathbf{r}_{c,N}$ is the rail irregularities vector in the normal direction. Note that the gap function $\mathbf{g}_{N}^{B}(x,t)$ between the bridge and auxiliary contact points (Fig. 1(b)) depends on both location x and time t, as $\mathbf{W}_{N}^{B}(x)$ matrix is time-dependent.

3.2 Earthquake motion constraints

Earthquake motion on the system is applied as an additional constraint equation to the bridge subsystem. This constraint equation is:

$$\bar{\mathbf{m}}^{B,g}\ddot{\mathbf{g}}^{B,g}+\bar{\mathbf{c}}^{B,g}\dot{\mathbf{g}}^{B,g}+\bar{\mathbf{k}}^{B,g}\mathbf{g}^{B,g}=\mathbf{0} \tag{22}$$

where $\mathbf{g}^{B,g}$ is the vector connecting the displacement at the bridge's supports with that of the ground:

$$\mathbf{g}^{B,g}=-\left(\mathbf{E}^{B,g}\right)^{\mathrm{T}}\mathbf{u}^{B}+\mathbf{q}^{g}. \tag{23}$$

and $\bar{\mathbf{m}}^{B,g}$, $\bar{\mathbf{c}}^{B,g}$ and $\bar{\mathbf{k}}^{B,g}$ are defined in Section 2.2. $\mathbf{q}^{g}(t)$ is the vector of the ground motion at the supports. Thus, the constraint equation (Eq. (22)) becomes:

$$\bar{\mathbf{K}}_{eff}^{B,g}\left(\mathbf{E}^{B,g}\right)^{\mathrm{T}}\mathbf{u}^{B}=\bar{\mathbf{K}}_{eff}^{B,g}\mathbf{q}^{g}. \tag{24}$$

This kind of treatment of earthquake excitation, i.e., as unique constraints at each support of the bridge, also allows the consideration of asynchronous ground motion at the bridge's supports as a future extension.

3.3 Constrain coefficients

This section calculates the mass $\bar{\mathbf{m}}_{N}^{V}$, $\bar{\mathbf{m}}_{N}^{B}$, $\bar{\mathbf{m}}^{B,g}$, damping $\bar{\mathbf{c}}_{N}^{V}$, $\bar{\mathbf{c}}_{N}^{B}$, $\bar{\mathbf{c}}^{B,g}$ and stiffness $\bar{\mathbf{k}}_{N}^{V}$, $\bar{\mathbf{k}}_{N}^{B}$, $\bar{\mathbf{k}}^{B,g}$ matrices of the motion constraints of Eqs. (19), (20) and (24). The calculation of the pertinent matrices involves first the definition of the direction of the corresponding constraints.

3.3.1 Vehicle system

The vector $\mathbf{b}_{i}^{V}$ defining the direction of the constraint between the vehicle and the auxiliary contact point i in the normal direction results from the contact direction matrices $\mathbf{W}_{N}^{V}$ and $\mathbf{E}_{N}^{V}$, and it is:

$$\mathbf{b}_{i}^{V}=\left(\left(\mathbf{W}_{N,i}^{V}\right)^{\mathrm{T}}\mathbf{W}_{N,i}^{V}+\left(\mathbf{E}_{N,i}^{V}\right)^{\mathrm{T}}\mathbf{E}_{N,i}^{V}\right)^{-1}\left[\left(\mathbf{W}_{N,i}^{V}\right)^{\mathrm{T}}\quad-\left(\mathbf{E}_{N,i}^{V}\right)^{\mathrm{T}}\right]. \tag{25}$$

In Eq. (25) subscript i refers to the column i of the contact direction matrices $\mathbf{W}_N^V$ and $\mathbf{E}_N^V$. In other words, $\mathbf{W}_{N,i}^V$ is the vector consisting of all entries of column i of $\mathbf{W}_N^V$ matrix, and similarly for $\mathbf{E}_{N,i}^V$. The mass matrix $\bar{\mathbf{m}}_N^V$, corresponding to the Lagrange multiplier $\boldsymbol{\lambda}_N^V$, is:

$$\bar{\mathbf{m}}_N^V = diag\left\{\mathbf{m}_{N,ii}^V\right\} \tag{26}$$

with:

$$\mathbf{m}_{N,ii}^V = \left(\mathbf{b}_i^V\right)^{\mathrm{T}} \begin{bmatrix} \mathbf{m}^V & \mathbf{0} \\ \mathbf{0} & \mathbf{m}^g \end{bmatrix} \mathbf{b}_i^V . \tag{27}$$

Accordingly, the damping $\bar{\mathbf{c}}_N^V$ and stiffness $\bar{\mathbf{k}}_N^V$ matrices are:

$$\bar{\mathbf{c}}_N^V = diag\left\{\mathbf{c}_{N,ii}^V\right\} \text{ and } \bar{\mathbf{k}}_N^V = diag\left\{\mathbf{k}_{N,ii}^V\right\} \tag{28}$$

where $\mathbf{c}_{N,ii}^V$ and $\mathbf{k}_{N,ii}^V$ are defined according to the characteristics of the system and of the time-integration algorithm.

3.3.2 Bridge system

Similar to the vehicle subsystem, the vector $\mathbf{b}_i^B$, defining the direction of the constraints between the bridge and the auxiliary contact point *i,* results from $\mathbf{W}_N^B$ and $\mathbf{E}_N^B$ contact direction matrices as:

$$\mathbf{b}_i^B = \left(\left(\mathbf{E}_{N,i}^B\right)^{\mathrm{T}} \mathbf{E}_{N,i}^B + \left(\mathbf{W}_{N,i}^B\right)^{\mathrm{T}} \mathbf{W}_{N,i}^B\right)^{-1} \left[\left(\mathbf{E}_{N,i}^B\right)^{\mathrm{T}} \quad -\left(\mathbf{W}_{N,i}^B\right)^{\mathrm{T}}\right]. \tag{29}$$

The mass matrix $\bar{\mathbf{m}}_N^B$, corresponding to the Lagrange multiplier $\boldsymbol{\lambda}_N^B$, is:

$$\bar{\mathbf{m}}_N^B = diag\left\{\mathbf{m}_{N,ii}^B\right\} \tag{30}$$

with:

$$\mathbf{m}_{N,ii}^B = \left(\mathbf{b}_i^B\right)^{\mathrm{T}} \begin{bmatrix} \mathbf{m}^g & \mathbf{0} \\ \mathbf{0} & \mathbf{m}^B \end{bmatrix} \mathbf{b}_i^B . \tag{31}$$

Accordingly, the damping $\bar{\mathbf{c}}_N^B$ and stiffness $\bar{\mathbf{k}}_N^B$ matrices are:

$$\bar{\mathbf{c}}_N^B = diag\left\{\mathbf{c}_{N,ii}^B\right\} \text{ and } \bar{\mathbf{k}}_N^B = diag\left\{\mathbf{k}_{N,ii}^B\right\} \tag{32}$$

where $\mathbf{c}_{N,ii}^B$ and $\mathbf{k}_{N,ii}^B$ are defined similarly to $\mathbf{c}_{N,ii}^V$ and $\mathbf{k}_{N,ii}^V$.

3.2.3 Ground motion

The direction of the constraints at the supports of the bridge results directly from $\mathbf{E}^{B,g}$ matrix:

$$\mathbf{b}_i^{B,g} = \left(\mathbf{E}_i^{B,g}\right)^{\mathrm{T}} . \tag{33}$$

The mass matrix $\bar{\mathbf{m}}^{B,g}$, corresponding to the Lagrange multiplier $\boldsymbol{\lambda}^{B,g}$, is:

$$\bar{\mathbf{m}}^{B,g} = diag\left\{\left(\mathbf{b}_i^{B,g}\right)^{\mathrm{T}} \mathbf{m}^B \mathbf{b}_i^{B,g}\right\} \tag{34}$$

and the damping $\bar{\mathbf{c}}^{B,g}$ and stiffness $\bar{\mathbf{k}}^{B,g}$ matrices are:

$$\bar{\mathbf{c}}_N^{B,g} = diag\left\{c_{N,ii}^{B,g}\right\},\ \bar{\mathbf{k}}_N^{B,g} = diag\left\{\mathbf{k}_{N,ii}^{B,g}\right\}. \tag{35}$$

where $\mathbf{c}_{N,ii}^{B,g}$ and $\mathbf{k}_{N,ii}^{B,g}$ are defined similarly to $\mathbf{c}_{N,ii}^{V}$ and $\mathbf{k}_{N,ii}^{V}$.

4. System of equations

Equations (8), (10), (14), (19), (20) and (24) can be written as a system of equations (Eq. (1)):

$$\begin{bmatrix} \mathbf{K}_{\text{eff}}^{V} & \mathbf{0} & \mathbf{W}_N^V \bar{\mathbf{K}}_{\text{eff},N}^{V} & \mathbf{0} & \mathbf{0} & \mathbf{0} \\ \mathbf{0} & \mathbf{K}_{\text{eff}}^{B} & \mathbf{0} & -\mathbf{W}_N^B \bar{\mathbf{K}}_{\text{eff},N}^{B} & \mathbf{0} & -\mathbf{E}^{B,g} \bar{\mathbf{K}}_{\text{eff}}^{B,g} \\ \bar{\mathbf{K}}_{\text{eff},N}^{V} \left(\mathbf{W}_N^V\right)^{\mathrm{T}} & \mathbf{0} & \mathbf{0} & \mathbf{0} & -\bar{\mathbf{K}}_{\text{eff},N}^{V} \left(\mathbf{E}_N^V\right)^{\mathrm{T}} & \mathbf{0} \\ \mathbf{0} & -\bar{\bar{\mathbf{K}}}_{\text{eff},N}^{B} & \mathbf{0} & \mathbf{0} & \bar{\mathbf{K}}_{\text{eff},N}^{B} \left(\mathbf{E}_N^B\right)^{\mathrm{T}} & \mathbf{0} \\ \mathbf{0} & \mathbf{0} & -\mathbf{E}_N^V \bar{\mathbf{K}}_{\text{eff},N}^{V} & \mathbf{E}_N^B \bar{\mathbf{K}}_{\text{eff},N}^{B} & \mathbf{m}^g \dfrac{d}{dt^2} & \mathbf{0} \\ \mathbf{0} & \bar{\mathbf{K}}_{\text{EFF}}^{B,g} \left(\mathbf{E}^{B,g}\right)^{\mathrm{T}} & \mathbf{0} & \mathbf{0} & \mathbf{0} & \mathbf{0} \end{bmatrix} \begin{bmatrix} \mathbf{u}^V \\ \mathbf{u}^B \\ \boldsymbol{\lambda}_N^V \\ \boldsymbol{\lambda}_N^B \\ \mathbf{u}^g \\ \boldsymbol{\lambda}^{B,g} \end{bmatrix} = \begin{bmatrix} \mathbf{F}^V - \mathbf{W}_T^V \mathbf{F}_x \\ \mathbf{F}^B + \mathbf{W}_T^B \mathbf{F}_x \\ \mathbf{0} \\ \mathbf{w}_N^B \\ \mathbf{F}^g \\ \bar{\mathbf{K}}_{eff}^{B,g} \mathbf{q}^g \end{bmatrix} \tag{36}$$

with:

$$\mathbf{w}_N^B = v^2 \bar{\mathbf{m}}_N^B \mathbf{r}_{c,N}'' + v \bar{\mathbf{c}}_N^B \mathbf{r}_{c,N}' + \bar{\mathbf{k}}_N^B \mathbf{r}_{c,N}. \tag{37}$$

This system of equations (Eq. (36)) is solved in a partitioned manner. First, the contact forces and the response of the auxiliary contact points are calculated by substituting the first two rows of the system into the last four rows of Eq. (36). Then, the response of the vehicle and the bridge results by substituting the contact forces and the response of the auxiliary contact points into their EOMs (first two rows of Eq. (36)). The study adopts the Newmark's beta method for the time-integration, with $\gamma = 1/2$ and $\beta = 1/4$ [20].

5. Numerical application

This section applies the proposed numerical scheme to a realistic vehicle-bridge system consisting of a series of ten simply supported bridges traversed by a 10-vehicle Pioneer train, similar to the study of Zeng and Dimitrakopoulos [4]. Each simply supported bridges is L = 32 m long, with mass per unit length m = 22.40 t/m, Young's modulus E = 35.5 GPa, section area A = 8.63 m^2, lateral flexural moment of inertia I_{zz} = 85.86 m^4, vertical flexural moment of inertia I_{yy} = 6.58 m^4, and torsional stiffness J = 15.21 m^4. The vehicle properties are derived by [4]. The vehicle runs on rails of "very good" quality of irregularities according to the German Spectra [2] at speed v = 300 km/h. When the vehicle enters the bridge, a strong earthquake (Fig. 3) strikes. Fig. 3 plots the vertical (Fig. 3(a)) and lateral (Fig. 3(b)) components of the acceleration history of

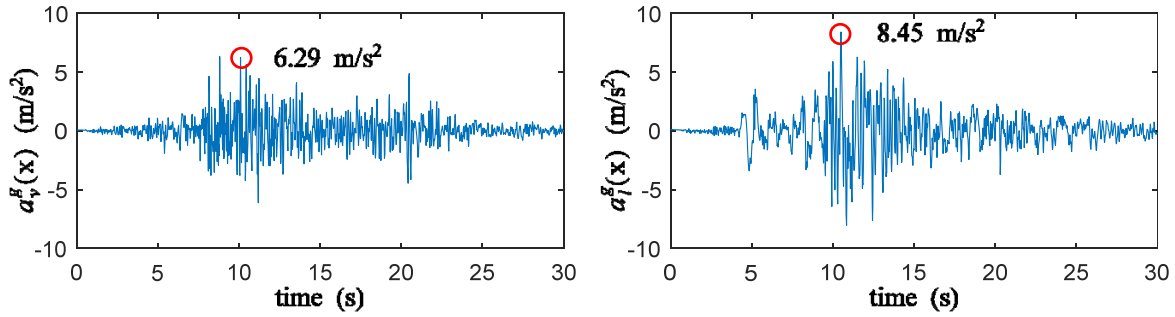

Fig. 3 – Acceleration time-histories of the Tabas earthquake motion: (a) vertical and (b) lateral components

the earthquake, recorded on September 16, 1978 at Tabas Station in Iran, [21].

The study solves the coupled VBI problem with the following methods: the proposed localized Lagrange multipliers approach with a dynamic representation of the Lagrange multipliers via ODEs (localized - dynamic Lagrange), the solution of the complete coupled system where the Lagrange multipliers are also treated dynamically (coupled - dynamic Lagrange), and the classic Lagrange multipliers method that solves the coupled problem as a system of high-index DAEs (coupled - classic Lagrange). Fig. 4 illustrates the response of the vehicle and the bridge in the normal and longitudinal directions for all three methods. The response at the midpoint of the first bridge (Fig. 4(a) and (b)) coincides in all cases. As expected, the longitudinal response of the bridge (Fig. 4(b)) is very small. The contact force of the first wheel of the tenth vehicle (Fig. 4(c)) is the same for the localized - dynamic Lagrange and coupled - dynamic Lagrange methods. The solution of the problem via a system of DAEs (coupled - classic Lagrange) results into numerical instabilities that create drifts mainly in the vehicle response. Thus, the contact force from the coupled – classic Lagrange method does not agree with the other two solutions. (Fig. 4(c)). The numerical drifts become more pronounced in the displacement of the car-body of the first vehicle (Fig. 4(e)). In this case, the coupled – classic Lagrange method shows very large drifts (Fig. 4(e)), while the localized – dynamic Lagrange and coupled – dynamic Lagrange algorithms are in perfect agreement (Fig. 4(f)).

The proposed localized – dynamic Lagrange approach that solves the vehicle and bridge subsystems separately is computationally more efficient than the coupled – dynamic Lagrange method, as it does not have to inverse the complete system matrix at each time step. For this 2D example, the proposed algorithm is 2 times faster than the coupled algorithm.

6. Conclusions

This study presents an original methodology to solve the SVBI problem consistently but also efficiently. Introducing auxiliary contact points between the vehicle' s wheels and the bridge, the analysis solves the vehicle and bridge subsystems separately. Based on the invariance of a generalized form of Newton's law, the proposed approach treats the dynamic Lagrange multipliers via second-order ODEs. This approach leads to the elimination of instabilities associated with DAE formulations. The study accounts for earthquake excitations via constraints between the displacement of the bridge and the ground motion at the supports.

The study applies the proposed numerical scheme to a realistic 2D vehicle-bridge configuration consisting of a ten-vehicle, HSR train traversing ten simply supported bridges subjected to a uniform earthquake excitation. In addition, it solves the same VBI problem with a coupled algorithm that treats Lagrange multipliers dynamically, as well as, with the classic Lagrange multipliers method, that considers kinematic constraints as algebraic equations, resulting into a system of high-index DAEs. The results indicate that the proposed approach is accurate, being in very good agreement with the coupled solution with a dynamic representation of Lagrange multipliers. Also, it is computationally more efficient compared to coupled algorithms. On the other hand, the classic Lagrange multipliers method shows large drifts, especially in the vehicle response.

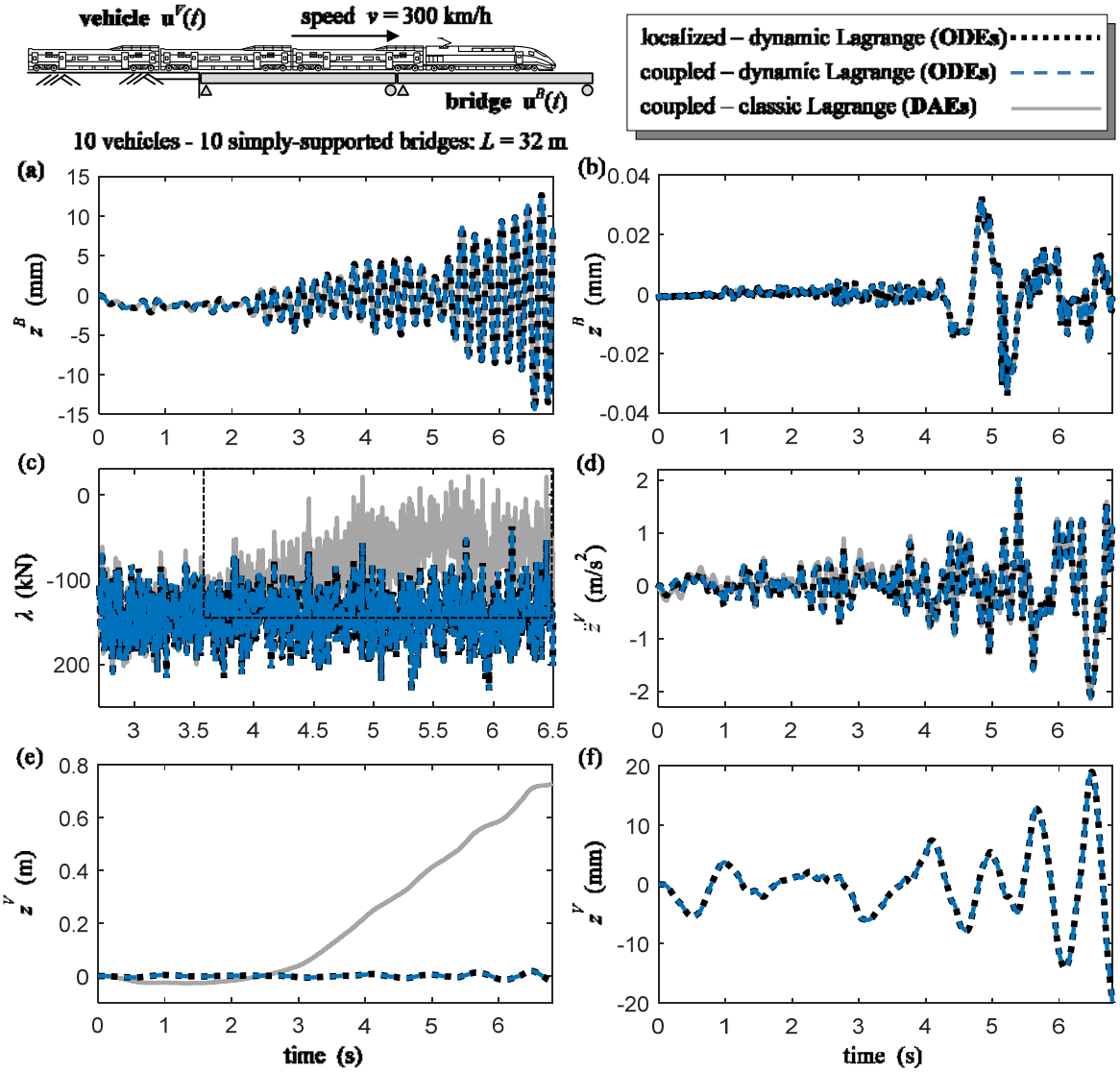

Fig. 4 – A ten-vehicle train running on ten simply supported bridges: (a) vertical and (b) longitudinal displacement at the midspan of the fist bridge, (c) contact force of the first wheel of the tenth vehicle, and (d) acceleration and (e-f) displacement of the car-body of the first vehicle, (e) with and (f) without the vehicle response from the DAEs solution.

The proposed approach is both accurate and computationally cheap, facilitating the treatment of large VBI problems in a consistent and efficient manner. This method can be extended to three-dimensional (3D) vehicle-bridge systems, while the application of earthquake via kinematic constraints at the bridge's supports enable the consideration of asynchronous ground motion to the bridge.

7. Acknowledgments

The first author would like to acknowledge the Hong Kong PhD Fellowship Scheme 2017/2018 (PF16-07238). The second author has received funding from the Hellenic Foundation for Research and Innovation (HFRI) and the General Secretariat for Research and Technology (GSRT), under Grant agreement No [617].

8. References

[1] He X, Wu T, Zou Y, Chen YF, Guo H, Yu Z (2017): Recent developments of high-speed railway bridges in China. *Structure and Infrastructure Engineering*, **13**(12), 1584-1595.

[2] Yang YB, Yau JD, Wu YS (2004): *Vehicle-Bridge Interaction: With Applications to High-Speed Railways*. World Scientific, Singapore.

[3] Zeng Q, Dimitrakopoulos EG (2016): Seismic response analysis of an interacting curved bridge-train system under frequent earthquakes. *Earthquake Engineering & Structural Dynamics*, **45**(7), 1129-1148.

[4] Zeng Q, Dimitrakopoulos EG (2018): Vehicle-bridge interaction analysis modeling derailment during earthquakes. *Nonlinear Dynamics*, **93**(4), 2315-2337.

[5] Yang YB, Lin BH (1995): Vehicle-bridge interaction analysis by dynamic condensation method. *Journal of Structural Engineering*, **121**(11), 1635-1643.

[6] Dimitrakopoulos EG, Zeng Q (2015): A three-dimensional dynamic analysis scheme for the interaction between trains and curved railway bridges. *Computers & Structures*, **149**, 43-60.

[7] Neves SGM, Azevedo AFM, Calçada R (2012): A direct method for analyzing the vertical vehicle-structure interaction. *Engineering Structures*, **34**, 414-420.

[8] Xia H, Zhang N, De Roeck G (2003): Dynamic analysis of high speed railway bridge under articulated trains. *Computers & Structures*, **81**(26), 2467-2478.

[9] Zeng Q, Stoura CD, Dimitrakopoulos EG (2018): A localized lagrange multipliers approach for the problem of vehicle-bridge interaction. *Engineering Structures*, **169**, 82-92.

[10] Yang YB, Wu YS (2002): Dynamic stability of trains moving over bridges shaken by earthquakes. *Journal of Sound and Vibration*, **258**(1), 65-94.

[11] Xia H, Han y, Zhang N, Guo W (2006): Dynamic analysis of train-bridge systems subjected to non-uniform seismic excitations. *Earthquake Engineering & Structural Dynamics*, **35**(12), 1563-1579.

[12] Du XT, Xu YL, Xia H (2012): Dynamic interaction of bridge-train system under non-uniform seismic ground motion. *Earthquake Engineering & Structural Dynamics*, **41**(1), 139-157.

[13] Petzold L (1982): Differential/algebraic equations are not ODE's. *SIAM Journal of Scientific and Statistical Computing*, **3**(3), 367-384.

[14] Baumgarte J (1972): Stabilization of constraints and integrals of motion in dynamical systems. *Computational Methods in Applied Mechanics and Engineering*, **1**(1), 1-16.

[15] Natsiavas S, Paraskevopoulos E (2015): A set of ordinary differential equations of motion for constrained mechanical systems. *Nonlinear Dynamics*, **79**(3), 1911-1938.

[16] Paraskevopoulos E, Natsiavas S (2013): On applications pf Newton's law to mechanical systems with motion constraints. *Nonlinear Dynamics*, **72**(1-2), 455-475.

[17] Géradin M, Cardona A (2001): *Flexible Multibody Dynamics: A Finite Element Approach*. Wiley, New York.

[18] Kalker JJ (1990): Variational and Numerical Theory of Contact, *Three-Dimensional Elastic Bodies in Rolling Contact* (137-184). Springer, Berlin.

[19] Shen ZY, Hedrick JK, Elkins JA (1983): A comparison of alternative creep force methods for rail vehicle dynamic analysis. *Vehicle System Dynamics*, **12**(1-3), 79-83.

[20] Newmark NM (1959): A method of computation for structural dynamics. *Journal of the Engineering Mechanics Division*, **85**(3), 67-94.

[21] PEERC database (2015): available at: https://ngawest2.berkeley.edu/site. Accessed May 2018.